Published in final edited form as:
Mol Microbiol. 2014 January ; 91(1): . doi:10.1111/mmi.12444.

Roles of the N domain of the AAA+ Lon protease in substrate recognition, allosteric regulation, and chaperone activity

Matthew L. Wohlever[1], **Tania A. Baker**[1,2], and **Robert T. Sauer**[1]

[1]Department of Biology, Massachusetts Institute of Technology Cambridge, MA 02139

[2]Howard Hughes Medical Institute, Massachusetts Institute of Technology Cambridge, MA 02139

Summary

Degron binding regulates the activities of the AAA+ Lon protease in addition to targeting proteins for degradation. The sul20 degron from the cell-division inhibitor SulA is shown here to bind to the N domain of *E. coli* Lon, and the recognition site is identified by crosslinking and scanning for mutations that prevent sul20-peptide binding. These N-domain mutations limit the rates of proteolysis of model sul20-tagged substrates and ATP hydrolysis by an allosteric mechanism. Lon inactivation of SulA *in vivo* requires binding to the N domain and robust ATP hydrolysis but does not require degradation or translocation into the proteolytic chamber. Lon-mediated relief of proteotoxic stress and protein aggregation *in vivo* can also occur without degradation but is not dependent on robust ATP hydrolysis. In combination, these results demonstrate that Lon can function as a protease or a chaperone and reveal that some of its ATP-dependent biological activities do not require translocation.

Keywords

ATP-dependent protease; degradation tag; allostery; protein aggregation

Introduction

An *Escherichia coli* cell contains more than 4000 different proteins, with wide variations in copy numbers. Under conditions that result in protein misfolding, about half of cytosolic protein degradation in *E. coli* is dependent on the AAA+ Lon protease (Chung and Goldberg, 1981). Lon appears to recognize some substrates by binding to degrons consisting largely of hydrophobic residues that are exposed as a consequence of unfolding or misfolding (Gur and Sauer, 2008). Lon also degrades natively folded proteins, including the SulA cell-division inhibitor, which contains an exposed C-terminal degron that is recognized by Lon (Higashitani *et al*., 1997; Gur *et al*., 2012). Lon proteases are present in most bacteria, in archaea, and in the endosymbiotic organelles of eukaryotes (Gur, 2013). Lon is necessary for rapid cell-cycle progression or pathogenicity in some bacteria, knockdown of mitochondrial Lon kills lymphoma cells, and overexpression of Lon increases fungal lifespan (Wright *et al*., 1996; Robertson *et al*., 2000; Ingmer and Brøndsted, 2009; Luce and Osiewacz, 2009; Bernstein *et al*., 2012; Breidenstein *et al*., 2012; Gora *et al*., 2013).

Like other AAA+ proteases, Lon sequesters its proteolytic active sites within a chamber, uses a hexameric ring and ATP hydrolysis to unfold and translocate proteins through a narrow axial pore into this chamber, and recognizes substrates predominantly by binding to degrons or peptide tags (Cha *et al*., 2010; Sauer and Baker, 2011). Unlike many AAA+ proteases, however, the AAA+ ATPase module and protease domain of Lon are part of a single polypeptide, and degron binding regulates Lon ATPase and protease activity in addition to serving a recognition function. For example, when otherwise identical proteins

are tagged with either the sul20 or β20 degron, which correspond respectively to the C-terminal 20 residues of SulA and a β-galactosidase sequence buried in the native protein, the maximal rate of *E. coli* Lon degradation can differ by 5 fold or more (Higashitani *et al*., 1997; Ishii and Amano, 2001; Gur and Sauer, 2008; 2009). These results suggest that degron binding shifts Lon into conformations with higher or lower protease activity.

In addition to its AAA+ module and peptidase domain, *E. coli* Lon contains a family-specific N domain that is necessary but not sufficient for hexamerization and has been proposed to be involved in substrate binding (Ebel *et al*., 1999; Roudiak and Shrader, 1998; 2000; Melnikov *et al*., 2008; Adam *et al*., 2012). Consistently, N-domain mutations or truncations result in defects in Lon activity *in vitro* (Cheng *et al*., 2012), but substrate binding to the N domain has not been directly demonstrated. Crystal structures (in non-native oligomeric states) are known for regions of the N domain, and recent electron-microscopy studies suggest that formation of Lon dodecamers is also mediated by the N domain (Li *et al*., 2005; 2010; Duman and Löwe, 2010; Vieux *et al*., 2013).

Here, we show that the sul20 degron binds to the N domain of *E. coli* Lon and identify mutations that define this binding site.. Degron binding to this site is not required for proteolysis of sul20-tagged substrates *in vitro* but enhances degradation by allosterically activating protease activity. Using additional Lon mutations that affect ATP hydrolysis, translocation, and proteolysis, we also probe the requirements for SulA inactivation and suppression of proteotoxic stress *in vivo*. SulA inactivation requires binding to the sul20-binding site in the N domain and ATP hydrolysis but does not require translocation or proteolysis. Lon-mediated relief of proteotoxic stress and protein aggregation can also occur without protein degradation but does not require robust ATP hydrolysis or a functional sul20-binding site in the N domain. In combination, our results show that *E. coli* Lon can function as a protease or as a chaperone, reveal that some biological activities do not require translocation through the axial pore, and support a model in which substrate binding to multiple sites on the Lon enzyme can alter its conformation and biological activities.

Results

The Lon N domain binds the sul20 degron

We initially sought to test if the sul20 degron binds to a site in the N domain of *E. coli* Lon. However, N-domain fragments do not form stable hexamers (Li *et al*., 2010), raising potential problems if substrate binding requires hexamerization or if interactions with hydrophobic surfaces normally buried in subunit-subunit interfaces create spurious non-specific binding. To circumvent these problems, we fused the Lon N domain to *E. coli* $ClpX^{\Delta N}$, a AAA+ enzyme that forms stable ring hexamers. $Chimera^{307}$ contained the entire Lon N domain (residues 1-307; Fig. 1A) fused to $ClpX^{\Delta N}$, whereas $chimera^{211}$ contained the first 211 residues of Lon, which included a globular region of the N domain but not an extended helical region (see, Fig. 2B). In addition, $chimera^{211}$ contained disulfide bonds between the subunits of $ClpX^{\Delta N}$, which have been shown to stabilize functional covalent hexamers (Glynn et al., 2012). Both chimeras supported degradation of an ssrA-tagged substrate in the presence of ClpP, the proteolytic partner of ClpX (Fig. 1B). As $ClpX^{\Delta N}$ hexamerization is required for functional interaction with ClpP (Stinson *et al*., 2013), these results confirm that both fusion proteins can assemble into active hexamers.

As assayed by changes in fluorescence anisotropy, $chimera^{307}$, $chimera^{211}$, and Lon^{S679A}, a variant with the active-site proteolytic serine mutated to alanine (Amerik *et al*., 1991), bound to a fluorescently labeled sul20 peptide with K_D's of ~2-5 μM, whereas $ClpX^{\Delta N}$ alone did not bind this peptide (Fig. 1C). The binding of $chimera^{211}$ and Lon^{S679A} to the fluorescent peptide was inhibited by an unlabeled sul20 peptide but not by a control peptide

(Fig. 1D). Thus, the sul20 peptide binds specifically to a site contained within the first 211 residues of the N domain of *E. coli* Lon.

Mapping the sul20 binding site

We attached a UV-activatable crosslinker that contained a biotin and cleavable disulfide to a sul20 "bait" peptide. Following incubation of the bait peptide with Lon, we activated crosslinking by UV irradiation, reduced the disulfide to remove the sul20 portion of the crosslinked moiety, cleaved with trypsin, and enriched for biotinylated peptides. Mass spectrometry identified a peptide with a mass (2022.8 Da) very close to that expected for Lon residues 100-113 plus the biotin label (2022.9 Da), suggesting that the sul20 binding site was within 14 Å (the linker length between the crosslinker and "bait") of this peptide. Next, we performed alanine-scanning mutagenesis of solvent-exposed residues within 14 Å of residues 100-113 in the crystal structure of an N-domain fragment (3LJC.pdb; Li *et al*., 2010). We mutated blocks of two or three residues, purified the variants, and assayed for defects in sul20-peptide binding by fluorescence anisotropy. Mutating residues 14-15, 33-35, or 36-38 to alanines resulted in substantial loss of binding (Fig. 2A). All of these residues were close in the 3LJC crystal structure, suggesting that all of these mutations affect the same binding site (Fig. 2B). We focused further studies on the R33A/E34A/K35A variant, henceforth called Lon$^{33\text{-}35}$, which had one of the largest defects in sul20 binding. Like the wild-type enzyme (Vieux *et al*., 2013), Lon$^{33\text{-}35}$ sedimented as a mixture of hexamers and dodecamers in analytical-centrifugation experiments (Fig. 2C).

An allosteric role for the sul20-binding site in the N domain

The sul20-binding surface in the N domain could be essential for efficient high-affinity tethering of sul20-tagged substrates to Lon prior to transfer to the translocation and degradation machinery or might function to enhance proteolytic activity of these substrates by an allosteric mechanism (Gur and Sauer, 2009). To distinguish between these possibilities, we assayed Lon$^{33\text{-}35}$ degradation of a set of model substrates that are degraded by wild-type Lon. These substrates included sul20- and β20-tagged derivatives of cp6-^{SF}GFP, a readily degraded circularly permuted variant of superfolder GFP, FITC-casein, a fluorescent β20 peptide, and sul20-tagged native and unfolded variants of the titin^{I27} domain (Gur and Sauer, 2008; 2009; Wohlever *et al*., 2013).

We initially assayed rates of Lon$^{33\text{-}35}$ and wild-type Lon degradation of different concentrations of cp6-^{SF}GFP-sul20 by monitoring changes in native fluorescence. Lon$^{33\text{-}35}$ degraded this substrate with a V_{max} ~20-fold lower than wild-type Lon but with a similar K_M (Fig. 3A; Table 1). This result supports an allosteric model in which sul20-degron binding to the 33-35 site in the wild-type N domain enhances proteolysis. It does not support a model in which the function of degron binding to the 33-35 sites is to increase the local concentration of a substrate that is then degraded directly by Lon, as this tethering model predicts an increase in the K_M for Lon$^{33\text{-}35}$ degradation of cp6-^{SF}GFP-sul20 but no change in V_{max}. We found that Lon$^{33\text{-}35}$ degraded β20-cp6-^{SF}GFP and FITC-casein with K_M and V_{max} values similar to wild-type Lon (Fig. 3B, 3C; Table 1), establishing that the 33-35 substitutions do not cause general defects in Lon degradation of all substrates. In combination, these results and experiments reported below support the existence of two types of binding sites for the sul20 degron; the N-domain sites defined by the 33-35 substitutions, which appear to mediate allosteric activation of protease activity upon sul20 binding, and a distinct site or sites responsible for determining the K_M for cp6-^{SF}GFP-sul20 degradation.

At low concentrations, some Lon substrates can activate degradation of other substrates with different degrons (Gur and Sauer, 2009). To test for an effect of the 33-35 mutations in this

transactivation assay, we monitored cleavage of a fluorescent β20 peptide by $Lon^{33\text{-}35}$ or wild-type Lon as a function of increasing concentrations of a non-fluorescent sul20-tagged protein, $titin^{I27}$-sul20. As shown in Fig. 3D, low concentrations of $titin^{I27}$-sul20 activated β20 cleavage by wild-type Lon, as expected for allosteric activation, whereas higher concentrations resulted in decreased cleavage, as expected for substrate competition for general proteolytic machinery. By contrast, $titin^{I27}$-sul20 activated $Lon^{33\text{-}35}$ β20 cleavage to a much smaller extent, supporting a role for sul20 binding to the 33-35 sites in the N domain in allosteric activation of protease activity.

$Lon^{33\text{-}35}$ hydrolyzed ATP at a rate ~2.5 slower than wild-type Lon in the presence of saturating cp6-^{SF}GFP-sul20 (Fig. 3E; Table 1). Modest decreases in the rate of ATP hydrolysis result in very slow degradation of GFP substrates by ClpXP (Martin *et al*., 2008a; Nager *et al*., 2011), and reduced ATPase stimulation probably amplifies the V_{max} defect for $Lon^{33\text{-}35}$ degradation of cp6-^{SF}GFP-sul20. Indeed, compared to wild type, $Lon^{33\text{-}35}$ showed smaller but still substantial V_{max} defects in degrading native $titin^{I27}$-sul20 and denatured CM-$titin^{I27}$-sul20 (Table 1), with the latter variant being unfolded by carboxymethylation of cysteines normally buried in the protein core. For these substrates, K_M for $Lon^{33\text{-}35}$ degradation was also increased compared to wild-type Lon (Table 1). Thus, the 33-35 mutations alter the kinetics of degradation of sul20-tagged substrates in ways that depend on properties of the tagged protein. Indeed, the K_M for sul20-tagged substrates by wild-type Lon can also vary substantially depending on the model substrate (Wohlever *et al*., 2013). No simple model allowed quantitative fitting of all of these experimental results, an unsurprising outcome given the complexity of this system.

Requirements for SulA inactivation in vivo

Inactivation of SulA by Lon is required for resumption of growth following repair of UV-induced DNA damage (Gottesman *et al*., 1981). To test the importance of different Lon activities in SulA inactivation, we used mutations that prevent or diminish specific biochemical functions. One mutation (S679A) prevents proteolysis by inactivating the peptidase active sites. We also used Lon variants expected to be defective in substrate translocation as a consequence of the Y398A mutation in the axial pore, variants expected to be defective in ATP hydrolysis as a consequence of the E424Q mutation in the Walker-B motif, and variants containing the 33-35 mutations. For these studies, wild-type Lon or mutant variants were cloned into low-copy plasmids, which were transformed into *E. coli* strains lacking the chromosomal *lon* gene. Following UV irradiation, plasmids expressing wild-type Lon, Lon^{S679A}, or $Lon^{Y389A/S679A}$ rescued growth (Fig. 4A). Western blots revealed that these Lon variants were expressed at levels similar to or slightly lower than chromosomal Lon (Fig. 4B). Overexpression of Lon^{S679A} was previously shown to inactivate SulA *in vivo* (Van Melderen and Gottesman, 1999). Our results confirm that Lon degradation is not required for SulA inactivation, even when the enzyme is expressed at cellular levels roughly comparable to normal cellular Lon levels. Our results also suggest that efficient translocation into the proteolytic chamber is unnecessary for inactivation, as $Lon^{Y389A/S679A}$ should be translocation defective. By contrast, the empty vector and plasmids expressing $Lon^{33\text{-}35}$, Lon^{E424Q}, and $Lon^{E424Q/S679A}$ failed to rescue growth (Fig. 4A), even though these variants were also expressed at levels similar to the other variants (Fig. 4B). Thus, Lon inhibition of SulA appears to require binding to the N-domain site defined by the 33-35 mutations as well as an activity affected by the E424Q mutation but not by the Y398A mutation.

To confirm that Lon^{Y398A} and Lon^{E424Q} were not defective in binding the sul20 degron and had the expected biochemical phenotypes, we purified both proteins and characterized their activities *in vitro*. Both mutants bound the sul20 peptide (Fig. 4C), with Lon^{E424Q} having

slightly higher affinity. Thus, the inability of Lon^{E424Q} and $Lon^{E424Q/S679A}$ to inactivate SulA *in vivo* is not correlated with a binding defect. As expected, Lon^{E424Q} displayed reduced rates of both basal and substrate-stimulated ATP hydrolysis (Fig. 4D). This reduced activity probably accounts for its inability to inactivate SulA. By contrast, Lon^{Y398A} had basal ATP-hydrolysis activity similar to wild-type Lon, but displayed substantially reduced rates of ATP hydrolysis in the presence of sul20- or β20-tagged substrates (Fig. 4D). Thus, a high level of substrate stimulation of ATPase activity does not appear to be important for SulA inactivation. Lon^{Y398A} did not degrade the unfolded CM-$titin^{I27}$-sul20 or CM-$titin^{I27}$-β20 substrates (Fig. 4E), a property consistent with the expected defect in translocation of substrates. Indeed, mutations analogous to Y398A in the axial pores of other AAA+ proteases also prevent substrate translocation and degradation (Siddiqui *et al*., 2004; Hinnerwisch *et al*., 2005; Park *et al*., 2005; Martin *et al*., 2008b). Lon^{E424Q} translocated and degraded CM-$titin^{I27}$-sul20 and CM-$titin^{I27}$-β20 at a very slow rate (Fig. 4F), suggesting that its very slow rate of ATP hydrolysis allows a correspondingly slow rate of proteolysis.

Suppression of proteotoxic stress occurs without degradation

We also tested the ability of different Lon variants to support growth of cells subjected to proteotoxic stress by high temperature, the absence of the chromosomal ClpXP and Lon proteases, and low levels of the DnaJ and DnaK chaperones (Tomoyasu *et al*., 2001). In this background at 42 °C, expression of wild-type Lon from a low-copy plasmid allowed robust growth, as did expression of $Lon^{33\text{-}35}$, Lon^{E424Q}, $Lon^{33\text{-}35/S679A}$, and $Lon^{E424Q/S679A}$ (Fig. 5A). Thus, degradation, robust ATP hydrolysis, and binding of client proteins to the sul20 site in the N domain are not required for Lon's ability to suppress proteotoxic stress. Expression of Lon^{S679A} provided partial rescue, whereas expression of $Lon^{Y398A/S679A}$ gave no rescue (Fig. 5A). The latter result suggests that substrate translocation is required for suppression of proteotoxic stress, although the inactivity of $Lon^{Y398A/S679A}$ could potentially arise from another defect conferred by the Y398A mutation (see Discussion). The plasmid-expressed Lon variants used in these assays were again expressed at levels similar to each other and to Lon expressed from its normal chromosomal location (Fig. 5B). We note that Lon^{S679A} was partially active, whereas $Lon^{33\text{-}35/S679A}$ and $Lon^{E424Q/S679A}$ were as active as wild-type Lon. These results suggest that the S679A mutation destabilizes the Lon conformation that is active in relieving stress, whereas the 33-35 and E424Q mutations stabilize this conformation. Indeed, Lon^{E424Q} bound the sul20 peptide ~5-fold more tightly than Lon^{S679A} (Fig. 1C, 4C), which could also reflect differential stabilization of different Lon conformations by these mutations. Notably, the Lon mutants that were active in inhibition of SulA were largely inactive in suppressing proteotoxic stress and *vice versa* (Fig. 4A, 5A), emphasizing that these activities occur by distinct mechanisms.

Under the conditions of the proteotoxic-stress assay, ~1.5% of intracellular proteins are recovered as insoluble aggregates both in *Δlon* and in *Δlon ΔclpXP* cells, which led to the proposal that Lon degrades misfolded proteins that accumulate when DnaK and DnaJ are limiting (Tomoyasu *et al*., 2001; Rosen *et al*., 2002). To test this model, we purified aggregated proteins from cells without Lon and cells expressing wild-type Lon, $Lon^{33\text{-}35/S679A}$, or $Lon^{E424Q/S679A}$. As monitored by SDS-PAGE and straining with Coomassie Blue, the levels of aggregated protein were comparable in cells expressing wild-type Lon and both proteolytically inactive double mutants and were substantially lower than the levels in cells with no Lon (Fig. 5C). Thus, Lon can suppress aggregation by a mechanism that does not require proteolysis, robust ATP hydrolysis, or the 33-35 N-domain sul20 binding site.

Discussion

The biochemical and genetic experiments described here provide evidence that the N domain of *E. coli* Lon binds the sul20 degron and this binding regulates proteolysis allosterically. A set of spatially adjacent residues in the N domain is required for efficient degradation of sul20-tagged substrates. For example, the 33-35 substitutions in the N domain dramatically weaken binding to a sul20 peptide, reduce V_{max} for degradation of sul20-tagged substrates, and prevent Lon relief of SulA inhibition of cell division following DNA damage. Lon$^{33\text{-}35}$ degrades some model substrates with steady-state kinetics similar to wild-type Lon, demonstrating that the 33-35 site is only required for the binding and/or efficient degradation of a subset of substrates. These mutations also prevent efficient transactivation of cleavage of a β20 peptide by a sul20-tagged protein, and alter stimulation of ATP hydrolysis by sul20-tagged substrates. These results support a model in which binding of the sul20 degron to the 33-35 site causes allosteric changes in the conformation of wild-type Lon that stimulate ATP hydrolysis and proteolysis. Although SulA is restricted to γ proteobacteria, Lon residues 33-35 are highly conserved across proteobacteria and Gram-positive bacteria, suggesting that this site serves to bind substrates with sul20-related degrons in these organisms.

The sul20 degrons of some cp6-^{SF}GFP-sul20 molecules are proteolytically clipped by Lon without global degradation, implying that the sul20 tag is the first segment of the substrate to pass through the axial pore and enter the degradation chamber (Wohlever *et al*., 2013). However, we find that the sul20 degron also binds to a distinct site in the N domain of Lon. Lon$^{33\text{-}35}$ degrades cp6-^{SF}GFP-sul20 with the same K_M as wild-type Lon, a fact inconsistent with a model in which the sul20 degron of this substrate initially binds to the N domain and is subsequently transferred to the axial pore. Rather, it appears that the sul20 degrons of some substrate molecules bind to the N domain and allosterically activate proteolysis of other substrate molecules whose degrons are independently engaged by the pore. Indeed, this model is supported by transactivation experiments reported here and previously (Gur and Sauer 2009). We also find that the Y398A mutation, which truncates a highly conserved aromatic side chain in the axial pore, prevents degradation of unfolded substrates bearing the sul20 or β20 degrons, dramatically reduces the maximal level of stimulation of ATP hydrolysis by these substrates, but does not impair binding of the sul20 degron to the N domain. These results are consistent with independent binding of sul20 degrons on different substrate molecules to the N domain and to the axial pore. Studies with other AAA+ proteases show that mutations corresponding to Y398A prevent or greatly slow the rate of substrate translocation (Siddiqui *et al*., 2004; Hinnerwisch *et al*., 2005; Park *et al*., 2005; Martin *et al*., 2008b). Thus, both allosteric activation via degron binding to the N domain and interaction of a translocating segment of polypeptide with the axial-pore loops appear to be required for normal coordination of substrate binding, ATP hydrolysis, and substrate translocation by Lon.

E. coli SulA, which inhibits cell division by binding to FtsZ (for review, see Löwe *et al*., 2004), can be inactivated by Lon in the absence of degradation. Van Melderen and Gottesman (1999) showed that overproduction of proteolytically inactive Lon^{S679A} rescued cell growth after UV irradiation, but Lon^{S679A} with a Walker-A mutation was not active in this assay. Because the Walker-A motif is required for ATP binding and hydrolysis, they proposed that Lon^{S679A} inactivates SulA by unfolding and translocating it into the inert proteolytic chamber of the mutant enzyme. Our results using Lon^{E424Q}, a Walker-B mutant, show that a robust level of ATP hydrolysis is required to inactivate SulA. However, Lon^{Y398A}, which appears to be defective in substrate translocation, is fully active in inhibiting SulA *in vivo*. Together, these results suggest that an activity, which depends upon robust ATP hydrolysis but not upon efficient substrate translocation, is required for

degradation-independent inhibition of SulA by Lon. The sul20 degron of SulA is not involved in FtsZ binding and should be accessible to Lon in the complex, based upon the crystal structure of *Pseudomonas aeruginosa* FtsZ•SulA (Higashitani *et al*., 1997; Cordell *et al*., 2003). It is possible, therefore, that Lon binds the sul20 degrons of one or more SulA molecules bound to FtsZ, with ATP hydrolysis then driving conformational changes in the N domains that allow Lon to strip SulA from FtsZ and prevent its rebinding. Indeed, regions of the Lon N domain have been shown to undergo nucleotide-dependent motions (Cheng *et al*., 2012).

Gur and Sauer (2009) found that the β20 degron, which is hydrophobic and likely to be similar to degrons in most misfolded proteins, stabilizes a Lon conformation with high ATPase activity and little or possibly no protease activity. In this conformation, they proposed that Lon unfolds β20-tagged substrates by translocating them through the axial pore but then releases them without degradation, giving misfolded proteins a chance to refold correctly. Although this model has not been ruled out, our SulA-inactivation results suggest that Lon can perform mechanical functions that require robust ATP hydrolysis but are not coupled to substrate translocation or degradation. Thus, the β20-stabilized conformation of Lon that hydrolyzes ATP rapidly may be one in which translocation-independent conformational changes can be coupled to protein remodeling reactions.

The Lon enzymes from yeast, mammals, and certain bacteria appear to mediate chaperone activity that is independent of proteolysis (Rep *et al*., 1996; Hori *et al*., 2002; Lee *et al*., 2004; Coleman *et al*., 2009). Indeed, in *E. coli*, we find that the protease-defective $Lon^{33\text{-}35/S679A}$ and $Lon^{E424Q/S679A}$ mutants suppress proteotoxic stress and protein aggregation as well as the wild-type Lon enzyme. Thus, proteolytically inactive Lon variants can function as chaperones, and wild-type Lon may also prevent aggregation of misfolded proteins by a degradation-independent mechanism. Many chaperones functions by binding to exposed hydrophobic patches in client proteins (Fenton *et al.*, 2004; Vabulas *et al.*, 2010), and such binding could also be important for Lon suppression of aggregation. Consistent with this model, the E424Q mutation dramatically reduces ATP hydrolysis but does not alter chaperone activity. If simple binding of misfolded proteins to Lon suppresses their aggregation, then the inactivity of $Lon^{Y398A/S679A}$ in the stress assay is likely to arise from perturbations in the binding of specific substrates in or near the axial pore, as homologous mutations in the pores of ClpX and ClpA reduce binding of specific degrons (Siddiqui *et al*., 2004; Hinnerwisch *et al*., 2005; Martin *et al*., 2008b). Alternatively, the low level of ATP hydrolysis mediated by Lon^{E424Q} may be sufficient to remodel misfolded proteins, allowing them to refold properly rather than aggregating. In this model, the inactivity of $Lon^{Y398A/S679A}$ could also be explained by its translocation defect. Because $Lon^{33\text{-}35/S679A}$ is fully active in the proteotoxic-stress assay, binding of the Lon N domain to sul20-like degrons does not appear to be important in suppressing protein aggregation.

Our present results and previous studies (Gur and Sauer, 2009) provide evidence for three distinct activities of *E. coli* Lon. These activities are likely to correspond to different conformations of the hexamer and/or dodecamer, with the binding of certain degrons stabilizing specific conformations. The proteolytic activity of Lon requires ATP-fueled translocation into the degradation chamber. Both hexamers and dodecamers have proteolytic activity, albeit with different substrate profiles (Vieux *et al*., 2013). Another activity, which mediates degradation-independent inactivation of SulA by variants such as $Lon^{Y398A/S679A}$, appears to involve remodeling that requires robust ATP hydrolysis but is translocation independent. A third activity suppresses aggregation of misfolded proteins by a degradation-independent mechanism that does not require robust ATP hydrolysis and may or may not involve translocation. The second and third activities are likely to correspond to different

enzyme conformations, but whether hexamers or dodecamers have both activities remains to be determined.

The family-specific N domains of the ClpX and ClpA AAA+ unfoldases serve as binding platforms for some substrates and adaptor proteins but can be deleted without compromising hexamer formation or robust degradation of certain substrates by ClpXP and ClpAP (Sauer and Baker, 2011). By contrast, the N domain of Lon is more highly integrated into overall enzyme architecture and function, including substrate binding, hexamer and dodecamer formation, and allosteric control of ATP hydrolysis and protease activity. Understanding in structural and dynamic terms how the N domain accomplishes these tasks is an important future challenge.

Materials and Methods

Protein cloning, expression, and purification

Variants of *E. coli* Lon were cloned into pBAD33 or a variant in which the chloramphenicol resistance marker of pBAD33 was replaced with an ampicillin resistance marker from pSH21. *E. coli* $ClpX^{\Delta N}$ and chimeras were cloned into HTUA vector and contained an N-terminal His_6 tag followed by a TEV protease site. $Chimera^{307}$ contained Lon residues 1-307, a two residue scar (EL, resulting from cloning into a Sac I restriction site), and $ClpX^{\Delta N}$ (residues 62-424 of wild-type ClpX). $Chimera^{211}$ contained Lon residues 1-211, a GSSG linker, the EL dipeptide, and $ClpX^{\Delta N}$. In addition, $chimera^{211}$ contained the C39S Lon mutation and C169S ClpX mutation to remove exposed cysteines and the ClpX T66C and P388C mutations to form inter-subunit disulfide bonds to stabilize hexamer formation (Glynn *et al*., 2012). ClpP was cloned into a pET22b vector with a His_6 tag on the C-terminus. $Titin^{I27}$ variants were cloned into a pSH21 vector with an N-terminal His_6 tag. β20-cp6-^{SF} GFP and cp6-^{SF}GFP-sul20 were cloned into a pCOLADuet1 vector with an N-terminal His_6 tag followed by a PreScission protease site. Mutations were generated either by QuickChange PCR (Stratagene) or by standard PCR techniques.

Lon was over-expressed with minor modifications from a method described previously (Wohlever *et al*., 2013). Briefly, cells were grown at 37 °C until OD_{600} = 1.0, induced with 0.2% arabinose at 37 °C for 3.5 h, harvested, and resuspended in LBA buffer [100 mM potassium phosphate (pH 6.5), 1 mM DTT, 1 mM EDTA, and 10% glycerol] to a final volume of 20 mL. Cells were incubated with lysozyme before sonication, and the crude cell lysate was cleared by high-speed centrifugation. The cleared lysate was incubated on ice for 20 min with 2 μL of benzonase (250 U/mL, Sigma) and then bound to P11 phosphocellulose resin (Whatman) equilibrated in LBA buffer. This resin was washed twice with LBA buffer and once with LBA buffer plus 100 mM potassium phosphate (pH 6.5). Lon was eluted from the P11 resin using LBA buffer plus 300 mM potassium phosphate (pH 6.5). The eluant was filtered to remove phosphocellulose, polyethyleneimine (PEI) was added to a final concentration of 0.12% to precipitate nucleic acids, additional phosphocellulose was added to remove excess PEI, and the mixture was filtered, concentrated, and chromatographed on an S200 column (GE Healthcare) equilibrated in 50 mM HEPES (pH 7.5), 2 M NaCl, and 1 mM DTT. Peak fractions from this column were pooled, buffer exchanged into storage buffer [50 mM HEPES (pH 7.5), 150 mM NaCl, 10 μM EDTA, 1 mM DTT, and 10% glycerol] and frozen at –80 °C.

E. coli ClpP, cp6-^{SF}GFP-sul20, β20-cp6-^{SF}GFP, and $titin^{I27}$ variants were expressed, purified, and carboxymethylated (if necessary) as described (Kenniston *et al*., 2003; Gur and Sauer, 2009; Glynn *et al*., 2012; Wohlever *et al*., 2013). For ^{35}S-labeling, cells were grown in a rich defined medium lacking methionine (TekNova) until OD_{600} = 0.6 , and ^{35}S-methionine (Perkin-Elmer) was added after 20 min of induction with 1 mM IPTG. ^{35}S-

labeled proteins were purified through the Ni-NTA step and then mixed at a 1:19 ratio with purified unlabeled substrate.

Cells expressing $ClpX^{\Delta N}$ and Lon-$ClpX^{\Delta N}$ chimeras were grown until OD_{600} = 1.0, induced with 1 mM IPTG for 3.5 h at room temperature, harvested, resuspended in lysis buffer [25 mM HEPES (pH 7.5), 400 mM NaCl, 100 mM KCl, 20 mM imidazole, 10% glycerol, and 10 mM 2-mercaptoethanol] to a total volume of 20 mL, and lysed by incubation with lysozyme and sonication. Following lysis, 2 μL of benzonase (250 U/mL, Sigma) and PMSF (final concentration 1 mM) were added, the lysate was cleared by high-speed centrifugation, and the supernatant was bound to Ni-NTA resin equilibrated in lysis buffer. The resin was washed with 30 mL of lysis buffer and eluted with lysis buffer plus 250 mM imidazole. For $ClpX^{\Delta N}$ and $chimera^{307}$, the eluant was chromatographed on S300 column (GE Healthcare) equilibrated in 50 mM Tris (pH 8.0), 300 mM KCl, 1 mM DTT, and 10% glycerol. Appropriate fractions were pooled, concentrated, and frozen at –80 °C. After elution of $chimera^{211}$ from the Ni-NTA resin, the protein was buffer exchanged into low-salt buffer [25 mM HEPES (pH 7.5), 50 mM KCl, 5 mM $MgCl_2$, 1 mM DTT, and 10% glycerol], incubated with 1 μM TEV protease for 90 min at room temperature to remove the His_6 tag, chromatographed on an S300 column as described above, and treated with copper phenanthroline to catalyze disulfide-bond formation between subunits as described (Glynn *et al*., 2012). The disulfide-bonded $chimera^{211}$ was purified on a Superose 6 column, concentrated, and frozen at –80 °C as described above, except in a buffer lacking DTT. Anti-Lon antibodies used for Western blots were a gift from the Baker lab (MIT).

Peptides

Peptides were synthesized, purified by reverse-phase HPLC, and masses were verified by mass spectrometry. The F-β20-Q peptide (sequence Z-QLRSLNGEWRFAWFPAPEAV-nY-A, where Z is a para-aminobenzoic acid fluorophore and nY is a nitrotyrosine quencher) was dissolved in dimethylsulfoxide and concentration was determined by absorbance (ε_{381} = 2200 M^{-1} cm^{-1}). The sul20 peptide (sequence ASSHATRQLSGLKIHSNLYH) was dissolved in 50 mM HEPES (pH 7.5) and concentration was measured by absorbance (ε_{280} = 1490). The sul20 peptide with an N-terminal fluorescein was dissolved in 25 mM Tris (pH 8.0) and concentration was determined by absorbance (ε_{495} = 83,397 M^{-1} cm^{-1}).

Biochemical assays

Unless noted, biochemical assays were performed in 25 mM Tris (pH 8.0), 100 mM KCl, 10 mM $MgCl_2$, at 37 °C using enzyme concentrations calculated for hexamer equivalents. Kinetic and anisotropy assays were performed in a SpectraMax M5 plate reader using 384-well clear plates (Corning) for absorbance assays and 96-well flat bottom ½-area plates (Corning) for fluorescence assays. ATPase assays contained supplemental 5 mM DTT, 2 mM ATP, lactate dehydrogenase (10 U/mL), and an ATP regeneration system [rabbit muscle pyruvate kinase (Sigma, 10 U/mL), 20 mM phosphoenolpyruvate (Sigma)]. The rate of ATP hydrolysis was measured by monitoring changes in absorbance at 340 nm, and reactions were initiated by the addition of $MgCl_2$ that had been pre-warmed to 37 °C. Degradation assays contained supplemental 1 mM DTT, an ATP regeneration system, and 2 mM ATP, which was used to initiate the reaction. Fluorescent substrates were incubated in plate reader until the fluorescence was constant prior to initiation of degradation. For degradation assays monitored by SDS-PAGE, 10 μL aliquots were taken at specified time points and mixed with 3.3 μL of 4X loading buffer [8% SDS, 250 mM Tris (pH 6.8), 40% glycerol, 160 mM DTT, and bromophenol blue]. The rate of degradation of ^{35}S-labeled $titin^{I27}$-sul20 variants was determined by measuring the amount of soluble radioactive products following precipitation with ice-cold trichloroacetic acid (Gottesman *et al*., 1998). The binding of fluorescent sul20 peptide to Lon^{S679A} and variants was measured in the

presence of 1 mM ATPγS to prevent substrate translocation; fluorescence anisotropy values were corrected for G-factor and scattering and fitted to a hyperbolic equation to determine a K_D value. Sedimentation-velocity ultracentrifugation was performed as described, except using proteolytically active $Lon^{33\text{-}35}$ (Vieux *et al*., 2013).

Cross-linking and mass spectrometry

Reactions were performed in the dark until the photo-activation step. The sul20 peptide (1 mM in 50 mM HEPES (pH 7.5), 150 mM NaCl, 10 μM EDTA, 10% glycerol) was incubated with 1 mM Sulfo-SBED (Pierce) for 30 min at room temperature, precipitated material was removed by centrifugation, and unreacted crosslinker was removed by dialysis using a 2 kDa MWCO membrane. The crosslinker-modified sul20 peptide (200 μM) was incubated with 10 μM Lon^{S679A} (hexamer equivalents), 1 mM ATPγS, and 1 mM $MgCl_2$ at room temperature for 5 min. Crosslinking was initiated by UV irradiation (365 nm) with a handheld lamp at a distance of 2 cm for 15 min. To reduce the disulfide bond linking the sul20 peptide to the crosslinker and Lon, 100 mM 2-mercaptoethanol was added and the reaction was incubated at room temperature for 1 h. Free sul20 peptide was removed by two consecutive microbio spin columns (BioRad). Labeling of Lon was verified by Western blotting with an anti-biotin antibody. The modified Lon protein was digested with sequencing grade trypsin (Roche) using a 1:100 enzyme:substrate ratio at 37 °C for 14 h, and cleavage was quenched with 1 mM TLCK. Biotinylated peptides were enriched by passage over a Monomeric Avidin Resin (Pierce) and were eluted from this column with 100 mM glycine buffer (pH 2.8). Samples were loaded onto a reverse phase protein trap, which was desalted on-line and eluted isocratically, and then analyzed by nanospray LC-MS using a QSTAR Elite quadrupole-time-of-flight mass spectrometer. Deconvolution of the electrospray data to generate molecular-weight spectra was performed with the BioAnalyst software included with the QSTAR Elite data system.

Biological assays

For assays of SulA inactivation *in vivo*, *E. coli* strain W3110 Δ*lon*::kan^R was transformed with pBAD33 or plasmid variants (cam^R) expressing wild-type Lon or Lon mutants. Cells were grown in Luria-Bertani (LB) broth to an OD_{600} of 0.9 – 1.3, diluted into fresh LB broth to an OD_{600} of 0.25, and 10-fold serial dilutions were prepared. 10 μL of each dilution was spotted onto an LB-agar plate containing 25 μg/mL kanamycin and 10 μg/mL chloramphenicol. The plate was exposed to 254 nm UV light from a handheld lamp at a distance of 5 cm for 10 s and was incubated overnight in the dark at 37 °C.

E. coli strain BB7357 expresses the DnaJ and DnaK chaperones from an IPTG-inducible promoter and lacks the chromosomal *lon*, *clpX*, and *clpP* genes (Tomoyasu *et al*., 2001). At 42 °C, BB7357 grows poorly when IPTG levels are low but an otherwise isogenic lon^+ strain grows well under these conditions. For proteotoxic-rescue assays, we transformed strain BB7357 with a pBAD33 variant encoding ampicillin resistance (empty vector) or derivatives expressing wild-type Lon or Lon mutants. Cells were grown at 30 °C in LB broth plus 1 mM IPTG until late-log phase, diluted to a final OD_{600} of 0.1, and serial 5-fold dilutions were prepared in LB broth. Small aliquots of each dilution were then spotted onto LB agar plates containing 25 μM IPTG, 25 μg/mL kanamycin, 10 μg/mL chloramphenicol, and 100 μg/mL ampicillin, and the plates were incubated overnight at 30 or 42 °C. For assays of protein aggregation, cells were grown at 30 °C in LB broth plus 100 μM IPTG to mid-log phase, the culture was split in two, grown for an additional 60 min at 30 or 42 °C, and then harvested. Aggregated proteins were purified by the method described by Tomoyasu *et al*. (2001), separated by SDS-PAGE, and visualized by staining with Coomassie Blue.

Acknowledgments

We thank B. Bukau, I. Levchenko, I. Papayannopoulos, E. Vieux, and members of the Sauer and Baker labs for reagents and helpful discussions, and D. Pheasant (MIT Biophysical Instrumentation Center) for help with the AUC experiments. T.A.B. is an employee of the Howard Hughes Medical Institute. This work was supported by N.I.H. grant AI-16982 and by an N.S.F. Graduate Research Fellowship to M.L.W.

References

Adam C, Picard M, Déquard-Chablat M, Sellem CH, Hermann-Le Denmat S, Contamine V. Biological roles of the Podospora anserina mitochondrial Lon protease and the importance of its N-domain. PLoS ONE. 2012; 7:e38138. [PubMed: 22693589]

Amerik AY, Antonov VK, Gorbalenya AE, Kotova SA, Rotanova TV, Shimbarevich EV. Site-directed mutagenesis of La protease. A catalytically active serine residue. FEBS Lett. 1991; 287:211–214. [PubMed: 1652461]

Bernstein SH, Venkatesh S, Li M, Lee J, Lu B, Hilchey SP, et al. The mitochondrial ATP-dependent Lon protease: a novel target in lymphoma death mediated by the synthetic triterpenoid CDDO and its derivatives. Blood. 2012; 119:3321–3329. [PubMed: 22323447]

Breidenstein EBM, Janot L, Strehmel J, Fernandez L, Taylor PK, Kukavica-Ibrulj I, et al. The Lon protease is essential for full virulence in Pseudomonas aeruginosa. PLoS ONE. 2012; 7:e49123. [PubMed: 23145092]

Cha SS, An YJ, Lee CR, Lee HS, Kim YG, Kim SJ, et al. Crystal structure of Lon protease: molecular architecture of gated entry to a sequestered degradation chamber. EMBO J. 2010; 29:3520–3530. [PubMed: 20834233]

Cheng I, Mikita N, Fishovitz J, Frase H, Wintrode P, Lee I. Identification of a region in the N-terminus of Escherichia coli Lon that affects ATPase, substrate translocation and proteolytic activity. J Mol Biol. 2012; 418:208–225. [PubMed: 22387465]

Chung CH, Goldberg AL. The product of the lon (capR) gene in Escherichia coli is the ATP-dependent protease, protease La. Proc Natl Acad Sci USA. 1981; 78:4931–4935. [PubMed: 6458037]

Coleman JL, Katona LI, Kuhlow C, Toledo A, Okan NA, Tokarz R, et al. Evidence that two ATP-dependent (Lon) proteases in Borrelia burgdorferi serve different functions. PLoS Pathog. 2009; 5:e1000676. [PubMed: 19956677]

Cordell SC, Robinson EJ, Löwe J. Crystal structure of the SOS cell division inhibitor SulA and in complex with FtsZ. Proc Natl Acad Sci USA. 2003; 100:7889–7894. [PubMed: 12808143]

Duman RE, Löwe J. Crystal structures of Bacillus subtilis Lon protease. J Mol Biol. 2010; 401:653–670. [PubMed: 20600124]

Ebel W, Skinner MM, Dierksen KP, Scott JM, Trempy JE. A conserved domain in Escherichia coli Lon protease is involved in substrate discriminator activity. J Bacteriol. 1999; 181:2236–2243. [PubMed: 10094703]

Fenton WA, Kashi Y, Furtak K, Horwich AL. Residues in chaperonin GroEL required for polypeptide binding and release. Nature. 1994; 371:614–619. [PubMed: 7935796]

Glynn SE, Nager AR, Baker TA, Sauer RT. Dynamic and static components power unfolding in topologically closed rings of a AAA+ proteolytic machine. Nat Struct Mol Biol. 2012; 19:616–622. [PubMed: 22562135]

Gora KG, Cantin A, Wohlever M, Joshi KK, Perchuk BS, Chien P, et al. Regulated proteolysis of a transcription factor complex is critical to cell cycle progression in Caulobacter crescentus. Mol Microbiol. 2013; 87:1277–89. [PubMed: 23368090]

Gottesman S, Halpern E, Trisler P. Role of sulA and sulB in filamentation by lon mutants of Escherichia coli K-12. J Bacteriol. 1981; 148:265–273. [PubMed: 7026534]

Gottesman S, Roche E, Zhou Y, Sauer RT. The ClpXP and ClpAP proteases degrade proteins with carboxy-terminal peptide tails added by the SsrA-tagging system. Genes Dev. 1998; 12:1338–1347. [PubMed: 9573050]

Gur E, Sauer RT. Recognition of misfolded proteins by Lon, a AAA(+) protease. Genes Dev. 2008; 22:2267–2277. [PubMed: 18708584]

Gur E, Sauer RT. Degrons in protein substrates program the speed and operating efficiency of the AAA+ Lon proteolytic machine. Proc Natl Acad Sci USA. 2009; 106:18503–18508. [PubMed: 19841274]

Gur E, Vishkautzan M, Sauer RT. Protein unfolding and degradation by the AAA+ Lon protease. Protein Sci. 2012; 21:268–278. [PubMed: 22162032]

Gur E. The Lon AAA+ protease. Subcell Biochem. 2013; 66:35–51. [PubMed: 23479436]

Higashitani A, Ishii Y, Kato Y, Koriuchi K. Functional dissection of a cell-division inhibitor, SulA, of Escherichia coli and its negative regulation by Lon. Mol Gen Genet. 1997; 254:351–357. [PubMed: 9180687]

Hinnerwisch J, Fenton WA, Furtak KJ, Farr GW, Horwich AL. Loops in the central channel of ClpA chaperone mediate protein binding, unfolding, and translocation. Cell. 2005; 121:1029–1041. [PubMed: 15989953]

Hori O, Ichinoda F, Tamatani T, Yamaguchi A, Sato N, Ozawa K, et al. Transmission of cell stress from endoplasmic reticulum to mitochondria: enhanced expression of Lon protease. J Cell Biol. 2002; 157:1151–1160. [PubMed: 12082077]

Ingmer H, Brøndsted L. Proteases in bacterial pathogenesis. Res Microbiol. 2009; 160:704–710. [PubMed: 19778606]

Ishii Y, Amano F. Regulation of SulA cleavage by Lon protease by the C-terminal amino acid of SulA, histidine. Biochem J. 2001; 358:473–480. [PubMed: 11513747]

Kenniston JA, Baker TA, Fernandez JM, Sauer RT. Linkage between ATP consumption and mechanical unfolding during the protein processing reactions of an AAA+ degradation machine. Cell. 2003; 114:511–520. [PubMed: 12941278]

Lee AY, Tsay SS, Chen MY, Wu SH. Identification of a gene encoding Lon protease from Brevibacillus thermoruber WR-249 and biochemical characterization of its thermostable recombinant enzyme. Eur J Biochem. 2004; 271:834–844. [PubMed: 14764100]

Li M, Gustchina A, Rasulova FS, Melnikov EE, Maurizi MR, Rotanova TV, et al. Structure of the N-terminal fragment of Escherichia coli Lon protease. Acta Crystallogr D Biol Crystallogr. 2010; 66:865–873. [PubMed: 20693685]

Li M, Rasulova F, Melnikov EE, Rotanova TV, Gustchina A, Maurizi MR, et al. Crystal structure of the N-terminal domain of E. coli Lon protease. Protein Sci. 2005; 14:2895–2900. [PubMed: 16199667]

Löwe J, van den Ent F, Amos LA. Molecules of the bacterial cytoskeleton. Annu Rev Biophys Biomol Struct. 2004; 33:177–198. [PubMed: 15139810]

Luce K, Osiewacz HD. Increasing organismal healthspan by enhancing mitochondrial protein quality control. Nat Cell Biol. 2009; 11:852–858. [PubMed: 19543272]

Martin A, Baker TA, Sauer RT. Protein unfolding by a AAA+ protease is dependent on ATP-hydrolysis rates and substrate energy landscapes. Nat Struct Mol Biol. 2008a; 15:139–145. [PubMed: 18223658]

Martin A, Baker TA, Sauer RT. Pore loops of the AAA+ ClpX machine grip substrates to drive translocation and unfolding. Nat Struct Mol Biol. 2008b; 15:1147–1151. [PubMed: 18931677]

Melnikov EE, Andrianova AG, Morozkin AD, Stepnov AA, Makhovskaya OV, Botos I, et al. Limited proteolysis of E. coli ATP-dependent protease Lon - a unified view of the subunit architecture and characterization of isolated enzyme fragments. Acta Biochim Pol. 2008; 55:281–296. [PubMed: 18506223]

Nager AR, Baker TA, Sauer RT. Stepwise unfolding of a β barrel protein by the AAA+ ClpXP protease. J Mol Biol. 2011; 413:4–16. [PubMed: 21821046]

Park E, Rho YM, Koh OJ, Ahn SW, Seong IS, Song JJ, et al. Role of the GYVG pore motif of HslU ATPase in protein unfolding and translocation for degradation by HslV peptidase. J Biol Chem. 2005; 280:22892–22898. [PubMed: 15849200]

Rep M, van Dijl JM, Suda K, Schatz G, Grivell LA, Suzuki CK. Promotion of mitochondrial membrane complex assembly by a proteolytically inactive yeast Lon. Science. 1996; 274:103–106. [PubMed: 8810243]

Robertson GT, Kovach ME, Allen CA, Ficht TA, Roop RM. The Brucella abortus Lon functions as a generalized stress response protease and is required for wild-type virulence in BALB/c mice. Mol Microbiol. 2000; 35:577–588. [PubMed: 10672180]

Rosen R, Biran D, Gur E, Becher D, Hecker M, Ron EZ. Protein aggregation in Escherichia coli: role of proteases. FEMS Microbiol Lett. 2002; 207:9–12. [PubMed: 11886743]

Roudiak SG, Shrader TE. Functional role of the N-terminal region of the Lon protease from Mycobacterium smegmatis. Biochemistry. 1998; 37:11255–11263. [PubMed: 9698372]

Rudyak SG, Shrader TE. Polypeptide stimulators of the Ms-Lon protease. Protein Sci. 2000; 9:1810–1817. [PubMed: 11045626]

Sauer RT, Baker TA. AAA+ proteases: ATP-fueled machines of protein destruction. Annu Rev Biochem. 2011; 80:587–612. [PubMed: 21469952]

Siddiqui SM, Sauer RT, Baker TA. Role of the processing pore of the ClpX AAA+ ATPase in the recognition and engagement of specific protein substrates. Genes Dev. 2004; 18:369–374. [PubMed: 15004005]

Stinson BM, Nager AR, Glynn SE, Schmitz KR, Baker TA, Sauer RT. Nucleotide binding and conformational switching in the hexameric ring of a AAA+ machine. Cell. 2013; 153:628–639. [PubMed: 23622246]

Tomoyasu T, Mogk A, Langen H, Goloubinoff P, Bukau B. Genetic dissection of the roles of chaperones and proteases in protein folding and degradation in the Escherichia coli cytosol. Mol Microbiol. 2001; 40:397–413. [PubMed: 11309122]

Vabulas RM, Raychaudhuri S, Hayer-Hartl M, Hartl FU. Protein folding in the cytoplasm and the heat shock response. Cold Spring Harbor Perspectives in Biology. 2010; 2:1–18.

Van Melderen L, Gottesman S. Substrate sequestration by a proteolytically inactive Lon mutant. Proc Natl Acad Sci USA. 1999; 96:6064–6071. [PubMed: 10339542]

Vieux EF, Wohlever ML, Chen JZ, Sauer RT, Baker TA. Distinct quaternary structures of the AAA+ Lon protease control substrate degradation. Proc Natl Acad Sci USA. 2013; 110:E2002–E2008. [PubMed: 23674680]

Wohlever ML, Nager AR, Baker TA, Sauer RT. Engineering fluorescent protein substrates for the AAA+ Lon protease. Protein Eng Des Sel. 2013; 26:299–305. [PubMed: 23359718]

Wright R, Stephens C, Zweiger G, Shapiro L, Alley MR. Caulobacter Lon protease has a critical role in cell-cycle control of DNA methylation. Genes Dev. 1996; 10:1532–1542. [PubMed: 8666236]

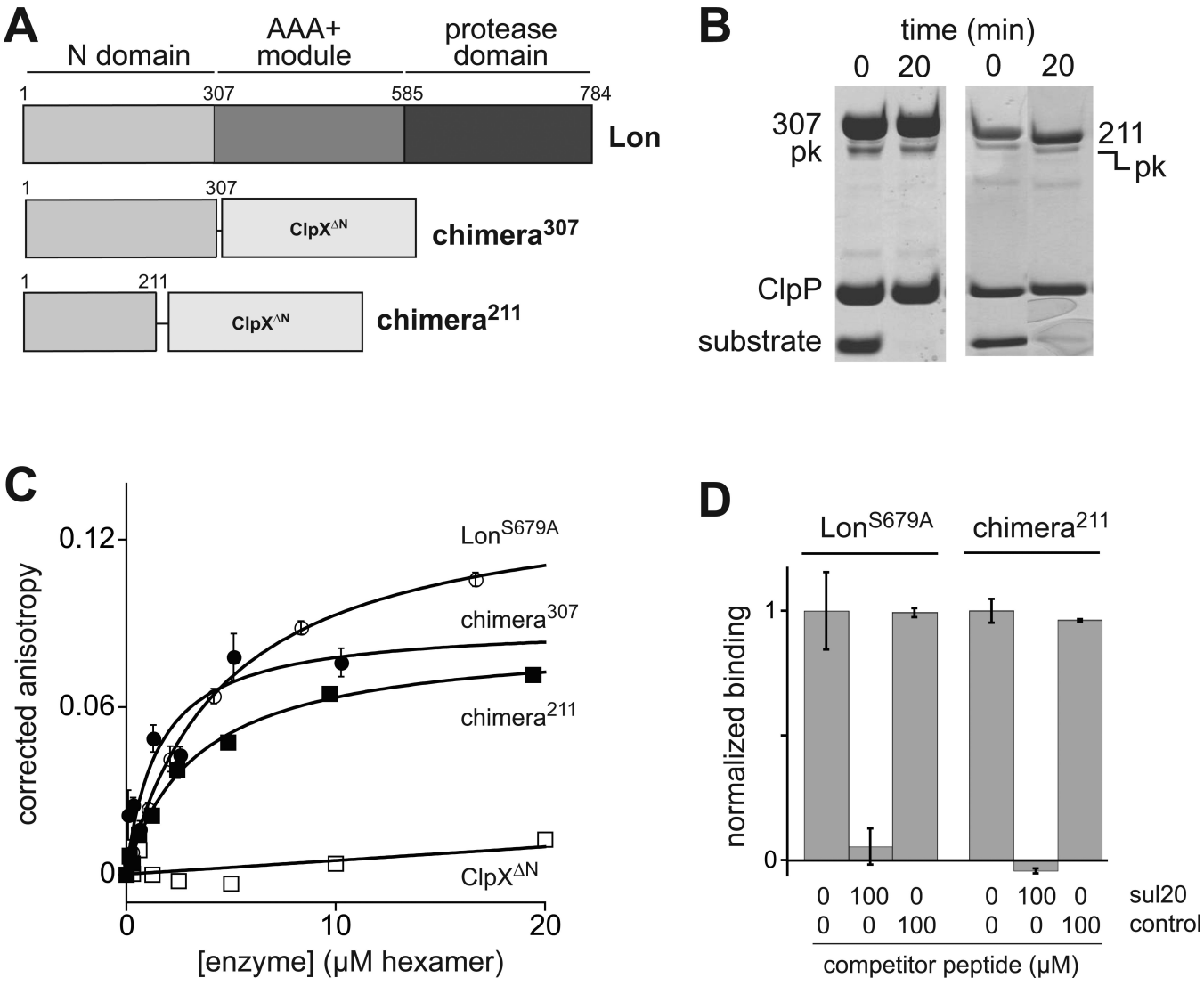

Figure 1.

The N domain of Lon binds the sul20 degron. (*A*) Domain organization of *E. coli* Lon and Lon-ClpX$^{\Delta N}$ chimeras. (*B*) In combination with *E. coli* ClpP, chimera^{201} or chimera^{307} supported degradation of CM-titin^{I27}-ssrA as assayed by SDS-PAGE. No substrate degradation was observed using ClpP alone. Pyruvate kinase (pk) was present for ATP regeneration. (*C*) Binding of a fluorescein-labeled sul20 peptide (200 nM) to Lon^{S679A}, chimera^{211}, chimera^{307}, or ClpX$^{\Delta N}$ was assayed by changes in fluorescence anisotropy (excitation 494 nm; emission 521 nm). Values are means ± SEM (N ≥ 2) after subtraction of the anisotropy of the free peptide. Solid lines are fits to a hyperbolic equation with fitted K_D's of 4.7 ± 0.2 μM (Lon^{S679A}), 3.4 ± 0.4 μM (chimera^{211}), and 1.5 ± 0.7 μM (chimera^{307}). (*D*) Binding of 160 nM fluorescent sul20 peptide to 6 μM Lon^{S679A} hexamer or binding of 80 nM fluorescent sul20 peptide to 6 μM chimera^{211} hexamer was assayed by anisotropy in the presence or absence of the specified concentrations of non-fluorescent sul20 peptide or an unrelated control peptide (KREHGAANDENYCLAA).

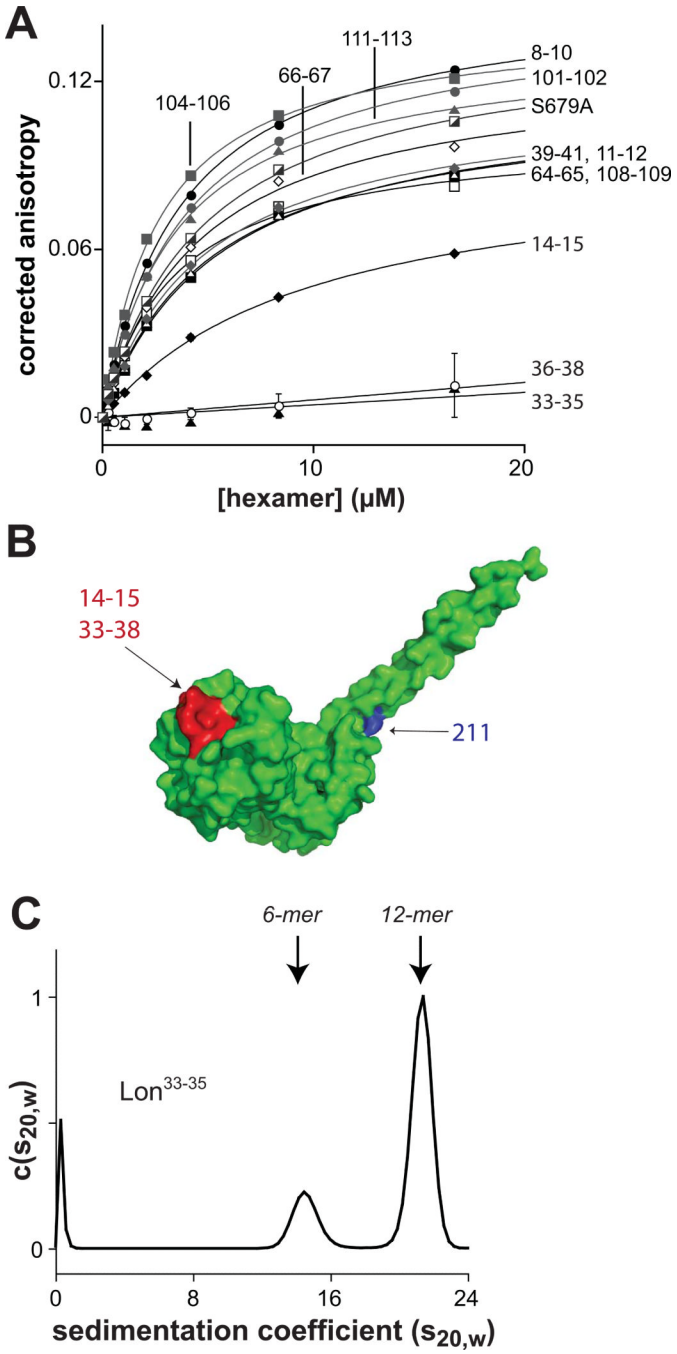

Figure 2.

Identification of the sul20 binding site in the Lon N domain. (*A*) Binding of fluorescein-labeled sul20 peptide to Lon^{S679A} or variants containing multiple alanine-substitution mutations was assayed by fluorescence anisotropy as described in the Fig. 1C legend. For clarity, error bars (± SEM; N = 3) are only shown for the mutants with severe defects in sul20 binding. (*B*) The positions of residues 14-15 and 33-38, which cause the largest defects in sul20 binding, are colored red in a surface representation of the crystal structure of part of the N domain (3LJC.pdb; Li *et al*., 2010). (*C*) Lon^{33-35} (3 μM hexamer equivalents) behaved as a mixture of hexamers and dodecamers in sedimentation velocity analytical ultracentrifugation performed at 20 °C and 16,000 rpm in 50 mM HEPES (pH 7.5), 150 mM

NaCl, 0.01 mM EDTA, 0.1 mM Tris (2-carboxyethyl) phosphine, 1 mM $MgCl_2$, and 0.1 mM ATPγS.

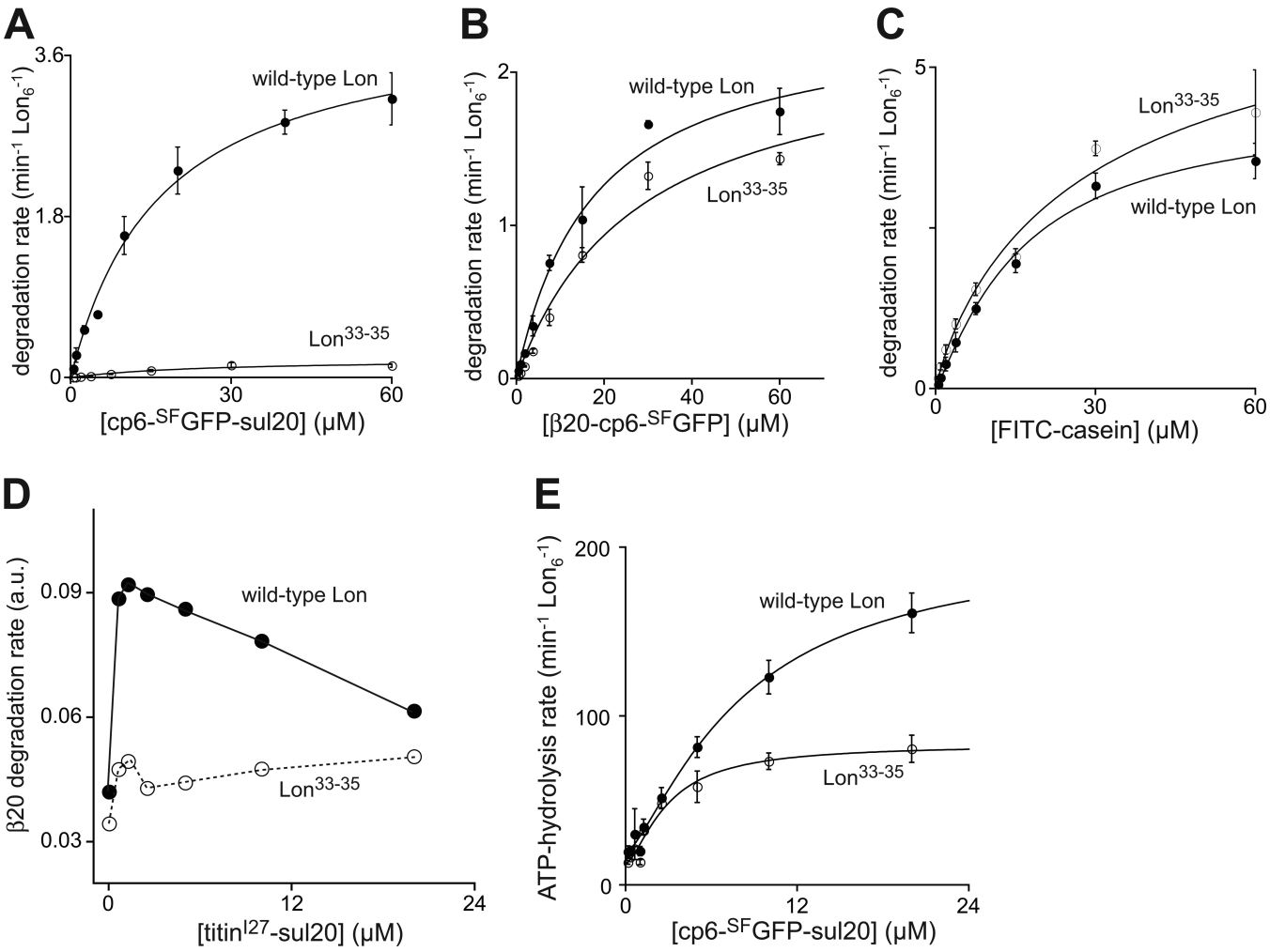

Figure 3.

Substrate degradation and ATP hydrolysis by Lon^{33-35} and wild-type Lon. (*A*) Degradation of different concentrations of cp6-^{SF}GFP-sul20 assayed by fluorescence (excitation 467 nm; emission 511 nm). Values are means ± SEM (N ≥ 2). (*B*) Degradation of different concentrations of β20-cp6-^{SF}GFP assayed by fluorescence (excitation 467 nm; emission 511 nm). Values are means ± SEM (N ≥ 2). (*C*) Degradation of different concentrations of FITC-casein (type II; Sigma) assayed by fluorescence (excitation 490 nm; emission 525 nm). Values are means ± SEM (N = 3). (*D*) Degradation of F-β20-Q peptide (2 μM) was assayed by fluorescence (excitation 320 nm; emission 422 nm) in the presence of increasing concentrations of titin^{I27}-sul20. Values are averages (N = 5). (*E*) ATP hydrolysis by wild-type Lon or Lon^{33-35} was assayed in the presence of difference concentrations of cp6-^{SF}GFP-sul20. In panels *A-C*, lines are fits to the Hill form of the Michaelis-Menten equation (rate = $V_{max}/(1+(K_M/[S]^n)$; see Table 1 for fitted parameters). In panel *E*, lines are fits to basal + amp/(1+(K_{app}/[S]^n), where V_{max} = basal + amp (see Table 1 for fitted parameters). Lon or Lon^{33-35} concentrations were 0.3 μM (hexamer equivalents) in panels *A-C* and 0.15 μM (hexamer equivalents) in panels *D-E*. The wild-type Lon data in panels *B-C* was taken from Wohlever *et al*. (2013).

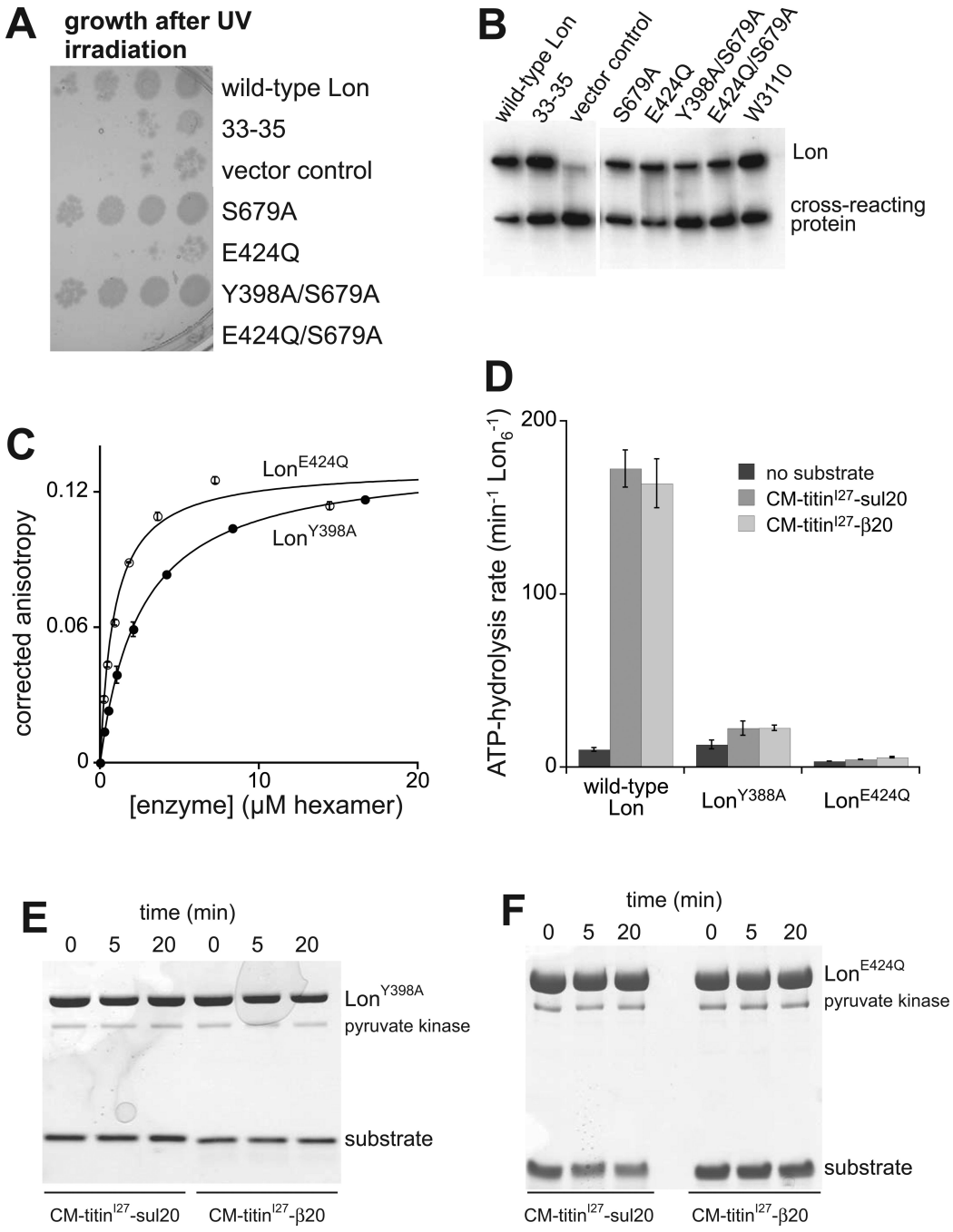

Figure 4.

Inactivation of SulA. (*A*) To monitor Lon-mediated inactivation of SulA, *E. coli* W3110 Δ*lon*::kan^R cells transformed with low-copy pBAD33 plasmids expressing Lon or Lon variants were irradiated with UV light, dilutions were spotted onto an LB agar plate, and the plate was incubated overnight at room temperature. (*B*) As assayed by SDS-PAGE and Western blotting with anti-Lon antibodies, chromosomal Lon in *E. coli* strain W3110 and Lon variants expressed from pBAD33 plasmids in strain W3110 Δ*lon*::kan^R were present at roughly similar intracellular levels following UV irradiation and 1 h of growth at room temperature. (*C*) Binding of Lon^{Y398A} (K_D = 2.6 ± 0.1 μM) and Lon^{E242Q} (K_D = 0.9 ± 0.1 μM) to the fluorescent sul20 peptide (200 nM). See Fig. 1C legend for conditions. (*D*) ATP

hydrolysis by wild-type Lon, Lon^{Y398A}, and Lon^{E424Q} (0.15 μM hexamer equivalents) was assayed in the absence of substrate or in the presence of CM-$titin^{I27}$-sul20 (20 μM) or CM-$titin^{I27}$-β20 (20 μM). (*E*) Lon^{Y398A} (0.6 μM hexamer equivalents) did not detectably degrade CM-$titin^{I27}$-sul20 (10 μM) or CM-$titin^{I27}$-β20 (10 μM) as assayed by SDS-PAGE. (*F*) Lon^{E424Q} (0.6 μM hexamer equivalents) degraded CM-$titin^{I27}$-sul20 (10 μM) or CM-$titin^{I27}$-β20 (10 μM) very slowly.

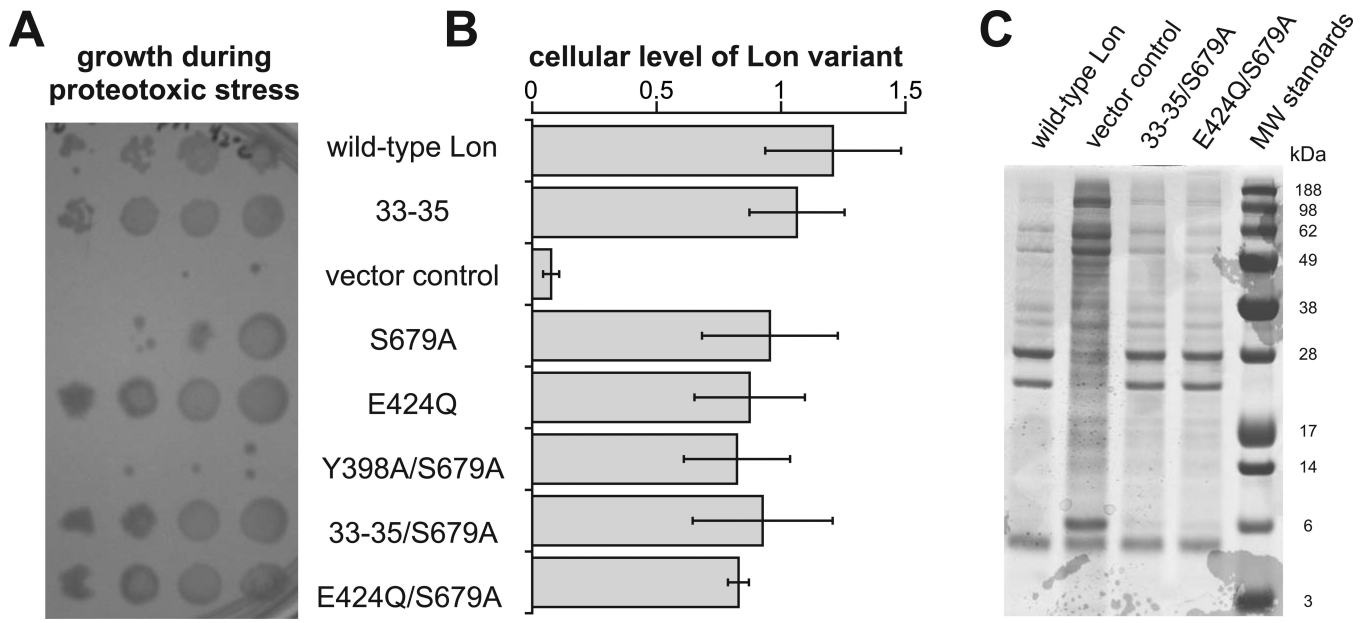

Figure 5.

Suppression of proteotoxic stress and aggregation *in vivo*. (*A*) Lon-mediated rescue of cells from proteotoxic stress caused by growth at 42 °C, under expression of DnaK and DnaJ, and deletion of the chromosomal genes for *lon*, *clpX*, and *clpP*. *E. coli* strain BB7357 was transformed with pBAD33 plasmids expressing wild-type Lon or Lon variants, dilutions were spotted onto LB agar plates, and plates were incubated at 42 °C for ~12 h. (*B*) Expression levels of mutants used in panel A were determined by Western blotting and densitometry and normalized to the average value of Lon in *E. coli* strain W3110. Values are averages ± SD (n ≥ 2). (*C*) Following growth for 1 h at 42 °C, aggregated proteins were purified from strain BB7357 transformed with an empty vector or with pBAD33 variants expressing wild-type Lon, $Lon^{33\text{-}35/S697A}$, or $Lon^{E424Q/S697A}$, and were visualized after SDS-PAGE by Coomassie-blue staining. The molecular weights of proteins in the SeeBlue* Plus2 standard mixture are shown (Life Technologies).

Table 1

Steady-state kinetic parameters

		protein degradation			ATP hydrolysis		
substrate	**Lon variant**	**V_{max} min^{-1} enz^{-1}**	**K_m (μM)**	**Hill constant**	**V_{max} min^{-1} enz^{-1}**	**K_{app} (μM)**	**Hill constant**
cp6-^{SF}GFP-sul20	wild type	3.6 ± 0.3	13 ± 2	1.2 ± 0.1	217 ±16	9.3 ± 1.3	1.2 ± 0.1
	33-35	0.15 ± 0.01	13 ± 2	1.2 ± 0.4	84 ± 13	3 ± 0.8	1.5 ± 0.6
P20-cp6-^{SF}GFP	wild type	2.3 ± 0.3	21 ± 6.0	1.2 ± 0.2	143 ± 5	2.6 ± 0.2	1.7 ± 0.1
	33-35	1.6 ± 0.1	14 ± 1.0	1.2 ± 0.2	nd	nd	nd
FITC-casein	wild type	4.4 ± 0.4	16 ± 4.0	1.2 ± 0.1	nd	nd	nd
	33-35	7.0 ± 2.0	31 ± 23	0.9 ± 2	nd	nd	nd
CM-titin^{I27}-sul20	wild type	17.1 ± 0.7	12 ± 1.0	1.4 ± 0.2	200 ± 20	0.6 ± 0.1	1.3 ± 0.4
	33-35	10.5 ± 0.4	70 ± 5.0	1.4 ± 0.1	270 ± 70	13 ± 10	0.7 ± 0.2
	Y398A	nd	nd	nd	23 ± 1	2.3 ± 0.5	3 ± 1.8
titin^{I27}-sul20	wild type	2.0 ± 0.1	29 ± 3.0	1.5 ± 0.2	118 ±5	1.0 ± 0.1	1.1± 0.1
	33-35	0.8 ± 0.3	80 ± 70	0.9 ± 0.2	79 ± 8	3.5 ± 0.9	1.2± 0.3
CM-titin^{I27}-β20	wild type	5.5 ± 0.1	18 ± 1.0	1.4 ± 0.1	174 ±7	1.6 ± 0.2	0.9 ± 0.1
	33-35	nd	nd	nd	250 ± 50	5.0 ± 3.0	0.7 ± 0.2
	Y398A	nd	nd	nd	25 ± 2	1.4 ± 0.4	1 ± 0.3

Errors are from non-linear-least-squares fitting. The wild-type data for cp6-^{SF}GFP-sul20 and cp6-^{SF}GFP-|β20 are from Wohlever *et al.* (2013). nd; not determined. K_{app} values represent the substrate concentration required for 50% stimulation of ATP hydrolysis. Basal rates of ATP hydrolysis in the absence of protein substrate were 10 ± 1 min^{-1} enz^{-1} (wild-type Lon), 10 ± 1 min^{-1} enz^{-1} (Lon$^{33\text{-}35}$), and 13 ± 3 min^{-1} enz^{-1} (Lon ^{Y398A}). Enzyme concentrations were calculated as hexamer equivalents.